Bioengineering

AIMS Bioengineering, 2(4): 335-374.
DOI: 10.3934/bioeng.2015.4.335
Received date 23 June 2015,
Accepted date 21 September 2015,
Published date 29 September 2015

http://www.aimspress.com/

Research article

ToMI-FBA: A genome-scale metabolic flux based algorithm to select optimum hosts and media formulations for expressing pathways of interest

Hadi Nazem-Bokaee and Ryan S. Senger*

Department of Biological Systems Engineering, Virginia Tech, Blacksburg, VA 24061, USA

* **Correspondence:** Email: senger@vt.edu.

Abstract: The Total Membrane Influx constrained Flux Balance Analysis (ToMI-FBA) algorithm was developed in this research as a new tool to help researchers decide which microbial host and medium formulation are optimal for expressing a new metabolic pathway. ToMI-FBA relies on genome-scale metabolic flux modeling and a novel *in silico* cell membrane influx constraint that specifies the flux of atoms (not molecules) into the cell through all possible membrane transporters. The ToMI constraint is constructed through the addition of an extra row and column to the stoichiometric matrix of a genome-scale metabolic flux model. In this research, the mathematical formulation of the ToMI constraint is given along with four case studies that demonstrate its usefulness. In Case Study 1, ToMI-FBA returned an optimal culture medium formulation for the production of isobutanol from *Bacillus subtilis*. Significant levels of L-valine were recommended to optimize production, and this result has been observed experimentally. In Case Study 2, it is demonstrated how the carbon to nitrogen uptake ratio can be specified as an additional ToMI-FBA constraint. This was investigated for maximizing medium chain length polyhydroxyalkanoates (mcl-PHA) production from *Pseudomonas putida* KT2440. In Case Study 3, ToMI-FBA revealed a strategy of adding cellobiose as a means to increase ethanol selectivity during the stationary growth phase of *Clostridium acetobutylicum* ATCC 824. This strategy was also validated experimentally. Finally, in Case Study 4, *B. subtilis* was identified as a superior host to *Escherichia coli*, *Saccharomyces cerevisiae*, and *Synechocystis* PCC6803 for the production of artemisinate.

Keywords: genome-scale model; microbial cell factory; flux balance analysis; *de novo* metabolic pathway

1. Introduction

1.1. Production of biofuels, valuable chemicals, and pharmaceuticals by microbial cell factories

A rapidly growing focus in the field of metabolic engineering is the construction of microbial cell factories (MCFs) that make use of engineered metabolic pathways for renewable production of biofuels, valuable chemicals, and pharmaceuticals. Recent examples using different microbial hosts include (among others): (i) isopropanol [1], 1-butanol [2], 3-methyl-1-butanol [3], styrene and aromatic building-blocks [4,5], glucaric acid [6], and 3-hydroxybutyrate [7] Taxol [8,9], astaxanthin [10,11], and artemisinin [12] using *Escherichia coli*; (ii) amino acids and poly 3-hydroxybutyrate using *Corynebacterium glutamicum* [13]; and (iii) isoprene production in cyanobacteria [14]. In addition, significant efforts are underway in pathway design and enzyme engineering that will ensure this approach continues to grow [15–18]. The issue of microbial host selection has also arisen as researchers look for different microbes to optimally express engineered pathways [19,20,21]. In particular, isobutanol production through the non-fermentative 2-keto acid route has now been studied in *E. coli* [22], *Synechocystis elongates* [23], *C. glutamicum* [24], *Bacillus subtilis* [25], *Saccharomyces cerevisiae* [26], and *Clostridium cellulolyticum* [27]. It is clear that new pathways are under development and represent a significant new phase in renewable production of chemicals. It is well established that a new pathway will require high availability of precursors and required cofactors; however, more information is needed about how to choose an optimal microbial host, genetic manipulation(s), and culture medium formulation to express this pathway highly. In this research, a new computational platform based on genome-scale metabolic flux modeling is introduced that can determine which microbial host(s) and media formulations can provide the required precursors and cofactors essential to optimize expression of any newly derived pathway. This approach can also be used as a starting point for the metabolic engineer to design genetic manipulation strategies.

1.2. Challenges of using non-platform hosts as microbial cell factories

Well-studied organisms, such as *E. coli*, are often chosen for expression of engineered pathways because their genetic engineering toolset(s) are well established. Given the exponential growth of high-throughput "-omics" datasets, the rapid advancements in molecular biology, the elucidation of enzyme kinetic parameters, and the automated methods for building genome-scale metabolic flux models, systems-level knowledge is becoming enriched on the physiology and biochemistry of lesser-studied organisms. It is conceivable that several of these organisms may ultimately be found superior for the expression of certain pathways, depending on precursors and cofactors required. However, the crucial challenges that exist currently are to (i) screen potential hosts for the expression of an engineered metabolic pathway and (ii) evaluate the optimal pathway use by the selected hosts. Certainly as the number of common microbial hosts increases in biotechnology, advances in evaluating the suitability of hosts for pathways requiring different precursors and cofactors are needed. Similarly, a "minimal cell" may also eventually emerge as a universal host in biotechnology. In this case, the addition of metabolic pathways to properly allocate precursors and cofactors to pathways of interest will be needed. With the advances in genome-scale metabolic flux modeling, it is proposed here that this problem may be best solved computationally.

1.3. Genome-scale models and the incorporation of new metabolic pathways in silico

Genome-scale metabolic flux models provide a snapshot prediction of steady-state metabolic activity and consist of a system of hundreds to thousands of linearized mass balance equations that are often solved using flux balance analysis (FBA) or flux variability analysis (FVA) with an objective function (i.e., maximizing the cell growth rate, among others) [28,29,30]. Thus, genome-scale metabolic flux models serve as platforms for efficient, fast, and holistic analyses of metabolism *in silico*. The number of reconstructed genome-scale models is growing rapidly, and the automated reconstruction resources have enabled the generation of draft models for any organism with a sequenced genome [31,32,33]. Additional tools, such as the Multi-Metabolic Evaluator (MultiMetEval), allow users to work with collections of metabolic models and even perform multi-objective analyses [34]. Thus, a systematic approach that allows incorporation of a new metabolic pathway into genome-scale models and further evaluates the potential use of that pathway is seen as a necesaary development. This was the motivation behind the creation of the Synthetic Metabolic Pathway Builder and Genome-Scale Model Database (SyM-GEM) (http://www.mesb.bse.vt.edu/SyM-GEM). The SyM-GEM web application allows the addition of user-created metabolic pathways to one or multiple genome-scale metabolic flux models of interest to biotechnology. The output of the SyM-GEM web application is a model compatible with the Systems Biology Markup Language (SBML) [35] that can be simulated using the COBRA Toolbox [36] in MATLAB. By combining the SyM-GEM and recently developed approach of Flux Balance Analysis with Flux Ratios (FBrAtio) [37,38], several metabolic engineering strategies (genetic manipulations) were installed in existing genome-scale models and evaluated for enhanced production of (i) cellulose from *Arabidopsis thaliana* using the AraGEM model [39]; (ii) isobutanol from engineered *S. cerevisiae* using iND750 model [40]; (iii) acetone from engineered *Synechocystis* PCC6803 using iJN678 model [41]; (iv) hydrogen from *E. coli* MG1655 using iAF1260 [42]; and (v) acetone, butanol, and isopropanol from engineered *C. acetobutylicum* using iCAC490 [37]. The results showed very good correlation between the experimental observations and the computational predictions. In some cases, the predictions introduced new and/or improved metabolic engneering strategies. However, in every case, it was not apparent that the host selected for pathway expression was, in fact, the optimal host or that the culture media had been formulated to ensure optimal expression. To address these questions, the Total Membrane Influx constrained Flux Balance Analysis (ToMI-FBA) algorithm was developed and is described in detail in the following sections.

1.4. ToMI-FBA: A computational framework for global evaluation of media formulations and metabolic pathway use in multiple hosts

The ToMI-FBA approach introduces a new stochastic set of constraints to the genome-scale metabolic flux model. In particular, ToMI-FBA allows the number of atoms that are imported into the *in silico* cell model (through any membrane transport process) to be constrained to a given value. This allows for a direct comparison of substrates (e.g., glucose vs. cellobiose) that contain different numbers of carbon atoms and allows different combinations of substrates to be imported simultaneously and compared directly. It also allows the exploration of common metabolic byproducts (e.g., acetate) for use as substrates. This new ToMI constraint is implemented by addition of new rows and columns to the stoichiometric matrix, similar (but not identical) to the FBrAtio

approach [37,38], and is discussed further below. In the stochastic approach used in ToMI-FBA, membrane transport processes of different potential carbon sources are enabled/disabled randomly so different combinations of transporters can be used simultaneously for the uptake of substrates and secretions of products. FBA is then applied with a constrained specific growth rate and the dual objectives of maximizing production of a targeted product while minimizing total flux in the metabolic network. The stochastic constraining of membrane transport reactions allows searching for all possible combinations of cofactors and precursors required for the engineered metabolic pathway to be used by the model. In other words, no prior knowledge or experimental observations are required about the physiology and biochemistry of cell metabolism prone to the new pathway. With ToMI-FBA, the whole process of adding a new pathway and evaluating its expression by multiple organisms and/or medium formulations *in silico* can be accomplished in a matter of hours. Performing the same task in laboratory requires skilled technicians, considerable time, and resources. The ToMI-FBA computational framework developed in this research assists researchers in generating systematic knowledge quickly before designing and implementing metabolic engineering strategies to optimize pathway expression. In this research, the ToMI-FBA method was applied to several genome-scale models with importance in biotechnology in four separate case studies to demonstrate its predictive capability. In particular, the case studies show (i) L-valine significantly improves the production of isobutanol from engineered *B. subtilis*, (ii) ethanol is the major fermentation product of cellobiose fermentation by *C. acetobutylicum* ATCC 824 at low pH, (iii) the carbon to nitrogen uptake ratio influences medium chain length polyhydroxyalkanoate (mcl-PHA) production from *Pseudomonas putida* KT2440, and (iv) *B. subtilis* is also a potential optimal host for the production of artemisinate. The ToMI-FBA algorithm is compatible with the COBRA Toolbox v2.0.5 [36] and is provided as a MATLAB function in the Supplementary Appendix to this manuscript.

2. Materials and Methods

2.1. Culture growth and analysis of metabolic substrates and products

C. acetobutylicum ATCC 824 was initially grown anaerobically on 2x YTG plates and later in liquid 2x YTG as described previously [43]. Culture growth was monitored by OD_{600}, and the cellobiose substrate and major metabolic products (i.e., acetate, butyrate, acetone, butanol, ethanol) were measured by HPLC using a previously developed method [43]. A Shimadzu HPLC (Shimadzu Co., Kyoto, Japan) was used along with an Aminex HPX-87H, 300 × 7.8 mm column (BioRad, Hercules, CA) for metabolite quantifications. Sulfuric acid (5 mM) was used as the isocratic mobile phase, and a constant flow rate of 0.5 mL/min was used. The column was maintained at 60˚C, detection was performed using refractive index, and the method was run for 35 minutes. To investigate the effects of cellobiose uptake during solventogenesis, the culture was grown to the onset of solventogenesis (OD_{600} = 3–3.5), cells were pelleted by centrifugation, and re-suspended in fresh 2x YTG (pH adjusted to 4.5) containing cellobiose substrate.

2.2. Software

All simulations were performed using MATLAB (R2012b) (MathWorks, Natick, MA) with the COBRA Toolbox v2.0.5 [36] and the open-source GLPK linear programming software. Standard FBA was used with the ToMI-FBA calculations. Both standard FBA and parsimonius FBA (pFBA) [44] were used as "traditional" FBA calculations in comparisons with ToMI-FBA. Both FBA and pFBA were run through the COBRA Toolbox v2.0.5. Genome-scale metabolic flux models were written in the Systems Biology Markup Language (SBML). To read and write SBML formatted models, the SBML Toolbox v4.1.0 and SBML library v5.8.0 were used [45]. The SyM-GEM database and web application (http://www.mesb.bse.vt.edu/SyM-GEM) was used to add metabolic pathways to genome-scale metabolic flux models of interest.

2.3. Genome-scale metabolic flux models, metabolic pathways, and the goals of case studies

In Case Study 1 of this research, the engineered metabolic pathway for the production of isobutanol from pyruvate through 2-ketoisovalerate intermediate developed by Atsumi et al. [22] (Figure 1a) was installed in the iBsu1103 model of *Bacillus subtilis* [46]. The goal of this case study was to use ToMI-FBA to determine what additional culture medium component(s) could further increase isobutanol production (Figure 1a). In Case Study 2, a genome-scale model of *P. putida* KT2440 was downloaded from the Model SEED [31]. Pathways to mcl-PHA from octanoate (Figure 1b) and acetyl-CoA (Figure 1c) were installed using SyM-GEM. ToMI-FBA with a constrained carbon to nitrogen uptake ratio was implemented to study this critical facet of culture medium design on mcl-PHA production. In Case Study 3, the iCAC490 model of *C. acetobutylicum* ATCC 824 [37] was updated to create the iCAC498 model, which is freely available through SyM-GEM. No additional pathways were added to this model, but ToMI-FBA was applied to determine which substrates and culture medium components impact acetone/butanol/ethanol (ABE) selectivity during the stationary phase of culture growth. Finally, in Case Study 4, the metabolic pathway for artemisinate production developed by Ro et al. [47] (Figure 1d) was added to the iAF1260 model of *E. coli* [42], the iBsu1103 model of *B. subtilis* [46], the iND750 model of *S. cerevisiae* [40], and the iJN678 model of *Synechocystis* PCC6803 [41]. The goal of this case study was to determine which of these hosts could achieve a higher artemisinate yield *in silico*.

2.4. Development and implementation of the ToMI constraint

The ToMI-FBA algorithm (i) locates all membrane transport reactions in a COBRA formatted genome-scale model, (ii) randomly sets directionality of unconstrained transport reactions, (iii) updates the stoichiometric matrix with the Total Membrane Influx (ToMI) constraint, (iv) constrains the specific growth rate to a specified value, (v) sets the new objective function of maximizing secretion of a targeted product, and (vi) performs FBA (or pFBA) given the new constraints and objective function. The entire sequence is repeated over a specified number of iterations (default = 1000), and the optimum solution, flux distribution, and constraints are retained. The ToMI constraint is implemented as follows. The ToMI value is assigned based on the total atom influx across the cell membrane. This means that by random assignment of transporters for influx or efflux, the size of the transported molecule(s) (i.e., number of carbon atoms in different carbohydrate sources) is taken into

account. The following is a mathematical description of ToMI. The quantity $A_{i,x}$ is the number of atoms of reactant *x* in reaction *i.* If there are *y* total reactants in reaction *i* and there are *j* total membrane transport reactions with constraints set to allow membrane influx only, the ToMI value is calculated according to Eq. 1. In general, the ToMI is defined as the total number of atoms in reactants of influx reactions multiplied by the flux values of those reactions.

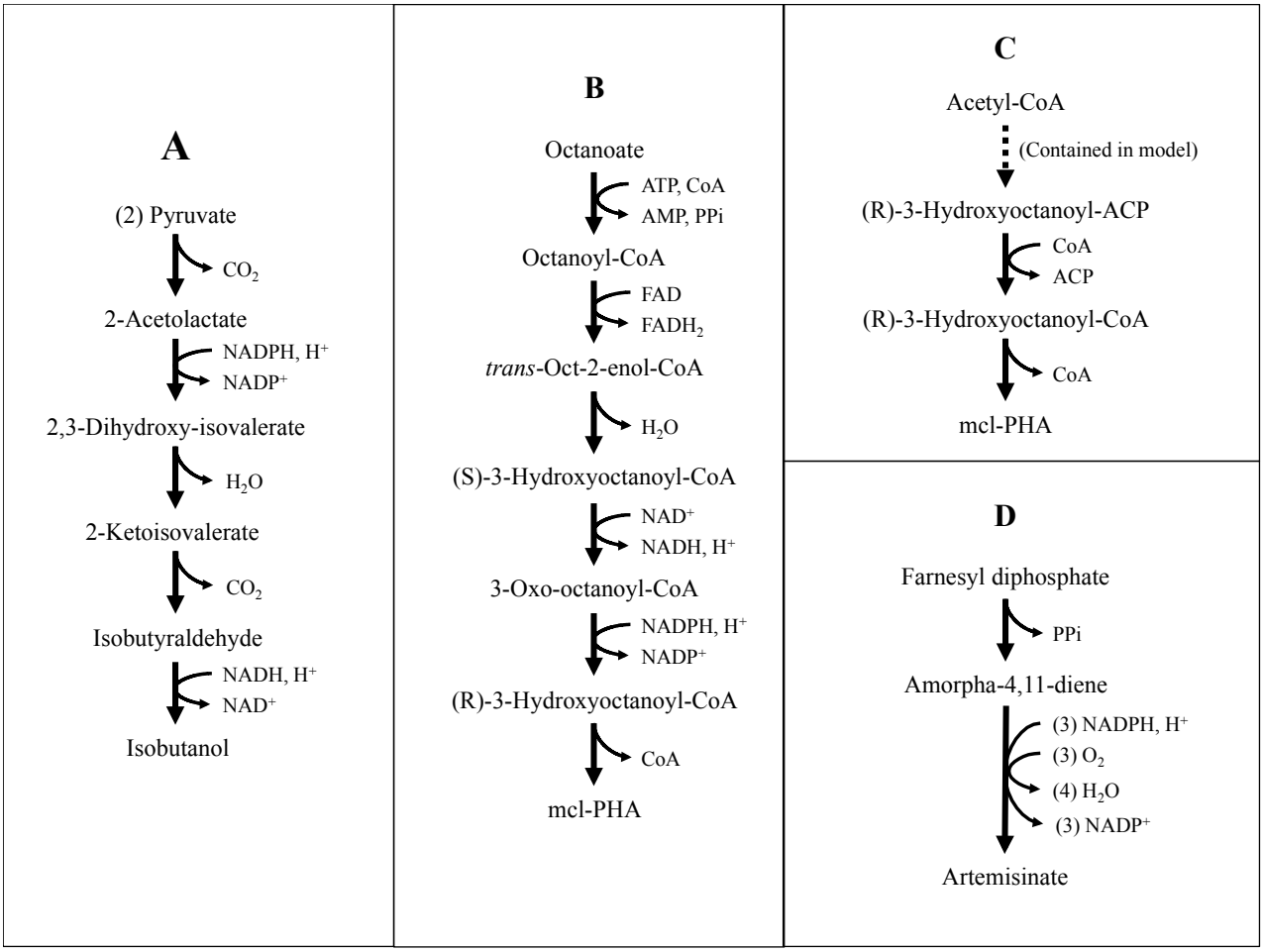

Figure 1. Metabolic pathways used as case studies in this research for the production of (A) isobutanol, (B and C) mcl-PHA, and (D) artemisinate.

$$ToMI = \sum_{x=1}^{y} \sum_{i=1}^{j} A_{i,x} v_i \qquad Eq.1$$

Not only can the ToMI value be calculated, it can also be specified and used as a constraint in a traditional genome-scale metabolic flux model (Eq. 2), where S is the $m \times n$ stoichiometric coefficient matrix and v is the vector of optimized flux values. To do this, Eq. 1 is re-arranged and set equal to zero, as shown in Eq. 3. To add the ToMI constraint to the stoichiometric matrix, the following steps are implemented: (i) add a new row and column to S, (ii) set the stoichiometric coefficient at $S_{m+1,n+1}$ equal to *–ToMI*, (iii) set the upper and lower constraints of the new reaction $n+1$ equal to 1, and (iv) in the new $m+1$ row of S, set the stoichiometric coefficient in columns corresponding to each membrane reaction (e.g., v_1) equal to the total number of atoms crossing the

membrane (e.g., $A_{1,1} + A_{1,2} + \cdots$). This procedure has been automated by the COBRA v2.0.5 compatible ToMI-FBA MATLAB function included in the Supplementary Appendix.

$$S \cdot v = 0 \qquad Eq.2$$

$$(A_{1,1} + A_{1,2} + \cdots)v_1 + (A_{2,1} + A_{2,2} + \cdots)v_2 + \cdots - ToMI = 0 \qquad Eq.3$$

The ToMI-FBA algorithm distinguishes among different transporters used by different genome-scale metabolic flux models and is also capable of finding the membrane transport reactions of multi-compartmental organismal models (i.e., the periplasm of *E. coli* models). When multiple compartments are included in a model, the membrane connected to the extracellular compartment is automatically considered for constraining ToMI.

2.5. Development and implementation of the carbon to nitrogen uptake ratio constraint

The carbon to nitrogen uptake ratio (CNR) can also be specified as a constraint in a genome-scale metabolic flux model ($S \cdot v = 0$) through the addition of a new row to the stoichiometric matrix, S. The definition of the CNR is defined in Eq. 4, where *j* is the number of reactions in the model, v_i represents the flux (membrane influx) of reaction *i,* C_i is the total number of carbon atoms transported in reaction *i*, and N_i is the total number of nitrogen atoms transported in this reaction. Eq. 4 is rearranged and set equal to zero (Eq. 5), and is further arranged to group terms by each v_i (Eq. 6). The constraint is added to S by adding an additional row to the matrix and then adding the stoichiometric coefficient $(C_i - CNR \cdot N_i)$ in each column corresponding to v_i. Unlike the ToMI constraint, the CNR constraint does not require the addition of a new column to S. This routine is included with the ToMI-FBA MATLAB function in the Supplementary Appendix.

$$CNR = \frac{\sum_{i=1}^{j} C_i v_i}{\sum_{i=1}^{j} N_i v_i} \qquad Eq.4$$

$$(C_1 v_1 + C_2 v_2 + \cdots) - CNR(N_1 v_1 + N_2 v_2 + \cdots) = 0 \qquad Eq.5$$

$$(C_1 - CNR \cdot N_1)v_1 + (C_2 - CNR \cdot N_2)v_2 + \cdots = 0 \qquad Eq.6$$

2.6. Development and implementation of the specific proton flux constraint

The specific proton flux (SPF) is a genome-scale metabolic modeling constraint originally developed by Senger and Papoutsakis [48] and specifies the total efflux of protons crossing the membrane of an *in silico* cell. The SPF includes the free protons in membrane transport reactions, but it also includes protons bound to acids that later deprotonate in the extracellular medium (i.e., acetic acid (acetate) and butyric acid (butyrate)). Thus, constraining the SPF in the presence of weak acids is more difficult than constraining the "exchange" flux of protons. The SPF constraint is implemented similarly to the ToMI constraint. In particular, the SPF is defined by Eq. 7, where *j* is the total number of reactions, P_i is the number of protons transported and v_i is the flux of the i^{th} membrane transport reaction.

$$SPF = \sum_{i=1}^{j} P_i v_i \qquad Eq.7$$

Like the ToMI constraint, the SPF constraint is added to the stoichiometric matrix by (i) re-arranging Eq. 7 (set equal to zero), (ii) adding a new row and column to the stoichiometric matrix, (iii) adding stoichiometric coefficients in the new row and columns that correspond to transport reactions and the SPF, and (iv) constraining the new SPF reaction to a flux value of 1. Similar to ToMI-FBA, the SPF constraint is compatible with the COBRA Toolbox v2.0.5 and COBRA formatted genome-scale metabolic flux models. A COBRA v2.0.5 compatible MATLAB function capable of implementing the SPF constraint is also included in the Supplementary Appendix.

3. Results

3.1. Case Study 1: L-Valine improves isobutanol production from B. subtilis

Isobutanol has attracted considerable attention as an advanced liquid biofuel because it has superior physical properties (e.g., energy density, hygroscopicity) to ethanol and has a higher octane number and is slightly less toxic to fermenting cultures than 1-butanol. After the introduction of the 2-keto acid pathway as a potential non-fermentative pathway to produce isobutanol in *E. coli* [22], there have been several metabolic engineering efforts to install this pathway in different hosts to enable isobutanol production from diverse substrates, including cellulose and CO_2/sunlight. Isobutanol yield from engineered *E. coli* was highest (0.41 g isobutanol per g glucose) when it was removed continuously from the cell culture broth to minimize product toxicity [49]. Higher tolerance has been shown by *C. glutamicum* [50] and especially *B. subtilis* (more than 2-fold increased product tolerance) [51]. It has also been shown experimentally that isobutanol production was enhanced significantly when L-valine was added to the culture medium of this organism [25]. The ToMI-FBA approach was implemented with a modified iBsu1103 model of *B. subtilis* to determine whether L-valine would be identified as a critical culture medium component to maximize isobutanol production.

The isobutanol pathway [22] (shown in Figure 1a) was added to the iBsu1103 model of *B. subtilis*. To do this, two new compounds (isobutyraldehyde and isobutanol) and four new reactions were added to iBsu1103. Two steps of this pathway (acetohydroxy acid isomeroreductase and dihydroxy acid dehydratase) were already present in the iBsu1103 model. ToMI-FBA was applied with the objective of maximizing isobutanol production at multiple constrained growth rates (from 0.1 to 0.5 h^{-1}). The ToMI values were varied from 0 to 500 mmol equivalent atoms $gDCW^{-1}$ h^{-1}. ToMI-FBA was applied with and without the possibility of importing L-valine from a minimal culture media (i.e., glucose, ammonia, O_2, and required minerals). The results of the ToMI-FBA simulations with allowed L-valine uptake are given in Figure 2a. The difference in isobutanol production given a minimal culture medium with L-valine and a minimal medium without L-valine is shown in Figure 2b. Based on these results, isobutanol production is directly correlated with ToMI and inversely correlated with the specific growth rate. In addition, significantly higher isobutanol production levels were observed when L-valine was included as a possible substrate. In all cases where L-valine could be imported (Figure 2a), ToMI-FBA found it beneficial to import L-valine. A complex medium formulation consisting of all carbon sources, amino acids, weak acids, nucleotides,

and cofactors present in the iBsu1103 model as simulated using ToMI-FBA. Here, L-valine uptake was also found to increase isobutanol production. To analyze the isobutanol pathway use, the ToMI-FBA simulations were repeated 10 times with random influx/efflux assignments to membrane transport reactions. At the end of each simulation, the iteration that resulted in the highest isobutanol flux was retained along with the network fluxes for that iteration. In order to find the optimum number of iterations for the modified iBsu1103 model, ToMI-FBA was run for 10, 30, 50, 100, and 1000 iterations (results not shown). With less than 50 iterations, the algorithm did not converge, and using more than 50 iterations returned identical results with the added computational expense. Thus, 100 iterations were used for the computational study, and all simulations showed isobutanol pathway use by iBsu1103. The average fluxes and standard deviations (over 10 ToMI-FBA simulations of 100 iterations each) of the isobutanol pathway for simulated growth on minimal media with L-valine and complex media are shown in Table 1 for the arbitrarily constrained ToMI of 300 mmol equivalent atoms $gDCW^{-1}$ h^{-1}, specific growth rate of 0.2 h^{-1}, and glucose uptake rate of 10 mmol $gDCW^{-1}$ h^{-1}. According to ToMI-FBA simulation results, a portion of L-valine was converted to 2-keto-isovalerate, which was further metabolized to isobutanol. Moreover, in 50% of simulations, 2-keto-isovalerate was converted to 2-isopropylmalate, which was further metabolized to leucine. The ideal sources of carbon and nitrogen were a combination of several amino acids (including isoleucine, leucine, methionine, proline, tryptophan, and tyrosine) and propionate. Nucleotides (such as AMP and CMP), citrate, and niacin were also necessary in most simulations to generate high yield. Potassium, calcium, magnesium, and iron were also essential for the growth *in silico*. It is noted that with complex growth medium and constrained glucose uptake, L-proline and propionate uptake were preferred over L-valine, suggesting additional room for complex medium development. Major byproducts, such as carbon dioxide and water, were intuitive simulation results. The iBsu1103 model also has the capability to produce acetoin from acetolactate; however, simulation results yielded no acetoin production *in silico*. These results are in agreement with the experimental findings [25,51]. Overall, ToMI-FBA successfully identified L-valine as a beneficial culture medium component, which has been verified experimentally.

Of course, it is important to consider the meaning of the results of this case study presented in Figure 2 and Table 1. During ToMI-FBA, the specific growth rate of the host is constrained while flux is maximized through the production pathway (and minimized over the entire metabolic network). This means that the results presented in Figure 2 and Table 1 represent the upper limits of what is possible. In reality, production and flux values will be less since the cellular objective is growth, not production. Thus, results from ToMI-FBA should be used to compare conditions for more or less production of a targeted metabolite, not to predict exact production rates. While ToMI-FBA has the capability of defining favorable conditions and hosts for production of a targeted chemical, clearly there is potential to combine ToMI-FBA with approaches that also suggest genetic manipulations as metabolic engineering strategies.

Next, it is important to compare the ToMI-FBA simulation results with traditional FBA simulation results. Here, the specific growth rate was constrained (e.g., $\mu = 0.2$ h^{-1}), the specific uptake of glucose was constrained (i.e., 10 mmol $gDCW^{-1}$ h^{-1}), and the formation of isobutanol was maximized. To be consistent with ToMI-FBA, all other membrane transport (and metabolite exchange) reactions were allowed to be reversible. The results from standard FBA did not favor L-valine uptake, and several transport reactions reached their upper or lower flux bound. Next, isobutanol production was constrained (i.e., 10 mmol $gDCW^{-1}$ h^{-1}), and pFBA was used to minimize

the total metabolic flux. This simulation did identify L-valine as an important media component for isobutanol production. However, it also erroneously identified 2-oxoglutarate, glycerol 3-phosphate, and acetoacetate as important substrates while secreting uncommon byproducts, such as glucose 6-phosphate. The ToMI-FBA approach called for the consumption of glucose, amino acids (including L-valine), trace minerals, and propionic acid (in a small amount) and led to the production of largely cell biomass, isobutanol, CO_2, and water.

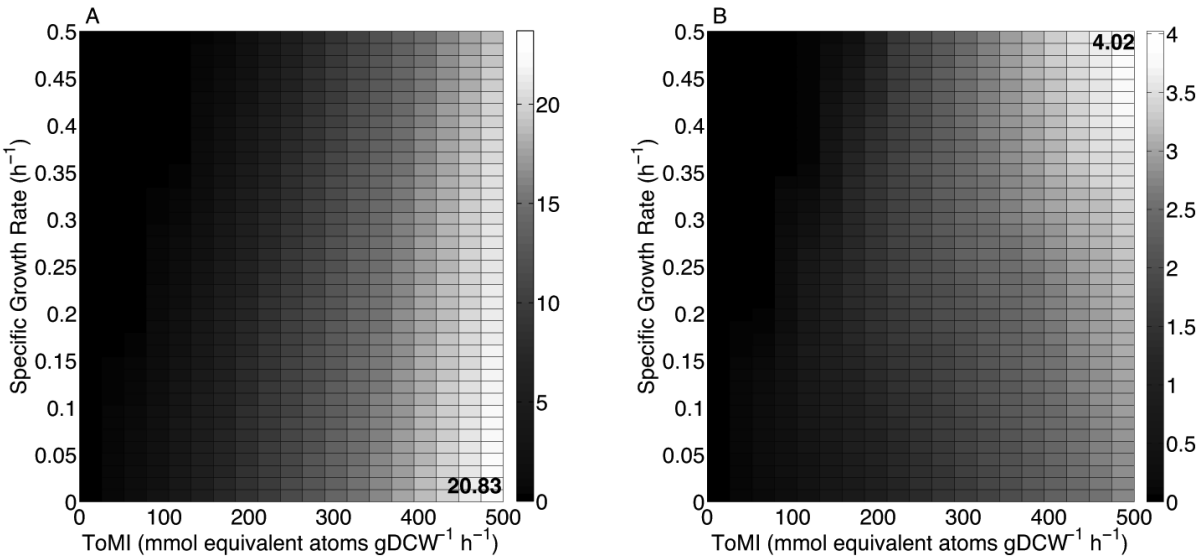

Figure 2. (A) Production of isobutanol (mmol gDCW^{-1} h^{-1}) from the modified iBsu1103 model of *B. subtilis* in the presence of minimal media supplemented with L-valine as a function of ToMI and the specific growth rate. (B) The additional flux that adding L-valine to minimal media provides over minimal media alone. The maximum values of each plot are given.

The ToMI-FBA approach limits the flux of atoms that can enter the cell through all transport reactions simultaneously. All metabolites with membrane transport reactions are available equally to the cell model, but the optimization selects only those that maximize isobutanol production. Thus, ToMI-FBA maximizes isobutanol production per atom entering the metabolic network. To do this effectively, reduced substrates are preferred, and these often appear as culture media components. Thus, the ToMI-FBA approach may be effective for designing culture media for the production of a desired product.

3.2. Case Study 2: The carbon to nitrogen uptake ratio influences mcl-PHA production by P. putida KT2440

It is known that nitrogen limitation leads to the onset of mcl-PHA production in *P. putida* KT2440. In addition, mcl-PHA can be produced from several carbon sources, but preferred and non-preferred sources do exist [52]. Starting with a genome-scale model downloaded from the Model SEED (and available on SyM-GEM), pathways to mcl-PHA through *de novo* fatty acid biosynthesis and β-oxidation (Figure 1b,c) were added using SyM-GEM. Next, the ToMI and CNR constraints

(Eqns. 3 and 6) were applied and varied, along with the specific growth rate, in ToMI-FBA simulations. Selected simulation results are shown in Figure 3, and mcl-PHA production was influenced by all three variables. In addition, an upper limit was established for the carbon to nitrogen uptake ratio at different values of ToMI (Figure 3a) and specific growth rate (Figure 3b). Beyond this boundary, growth and mcl-PHA production were infeasible. Simulations were run in the presence and absence of the preferred substrate for mcl-PHA production, octanoate. The preference for octanoate increased maximum mcl-PHA production by only about 1%, but its use minimized total flux of the metabolic network. Through the ToMI-FBA simulations, preferred substrates were identified as those often-used in "optimum" solutions. These are listed in Figure 3d. Octanoate was identified through ToMI-FBA simulations as the most preferred substrate, and this is consistent with experimental findings [52]. When traditional FBA was applied to this problem, the CNR constraint was critical to simulate mcl-PHA production. In addition, returning a set of preferred substrates consistent with the literature was not possible with FBA or pFBA, even with the CNR constraint installed. This case study also demonstrates the value of the CNR constraint in establishing the feasible phenotypic space, which is critical for culture medium design when nutrient limitation elicits production of a desired product.

3.3. Case Study 3: Cellobiose fermentation increases ethanol selectivity in C. acetobutylicum

The Gram-positive anaerobe *C. acetobutylicum* ATCC 824 is of considerable research interest due to its ability to convert a wide range of substrates to ABE products [43,53]. This organism undergoes a genetically programed metabolic shift where acids (i.e., acetate and butyrate) are produced during the exponential growth phase followed by acid re-uptake and conversion to ABE products during the stationary phase of culture growth. Senger and Papoutsakis developed the concept of the SPF and investigated its role in the metabolic shift in their original genome-scale modeling research of *C. acetobutylicum* [48,54]. In general, with a favorable proton motive force between the cytosol and extracellular environment, the cell can secrete acids (which is preferred). With a low medium pH, the cell must secrete solvents instead. ToMI-FBA was applied in this case to determine what substrate(s) could influence ABE selectivity when the SPF was constrained to mimic low medium pH. Butanol and acetone were highly coupled and maximized by butyrate uptake (which is well known). Ethanol, on the other hand, was maximized by cellobiose uptake during solventogenesis, a non-intuitive result. Traditional FBA, with and without the SPF constraint, was applied to see if a similar result could be obtained. Without the SPF constraint, FBA and pFBA returned lactate and 2-oxoglutarate as substrates to boost ethanol production during the stationary phase of growth. With the SPF constraint installed, FBA and pFBA returned mixtures of glucose and acetate. No case returned the same result (i.e., cellobiose) as the ToMI-FBA approach with the SPF constraint.

This ToMI-FBA simulation result was tested experimentally by (i) growing *C. acetobutylicum* to the onset of the stationary phase, (ii) separating cells from culture media (i.e., acetate and butyrate), and (iii) re-suspending cells in fresh culture media (pH adjusted to 4.5) with either a glucose or cellobiose substrate. As shown in Figure 4, cellobiose was converted to ethanol under these conditions and glucose was not, confirming the ToMI-FBA simulation result. It is noted that acid products were still produced by the experimental culture with the addition of cellobiose (glucose was

converted primarily to acids). However, this culture receiving cellobiose accumulated nearly twice as much ethanol during the stationary phase of growth.

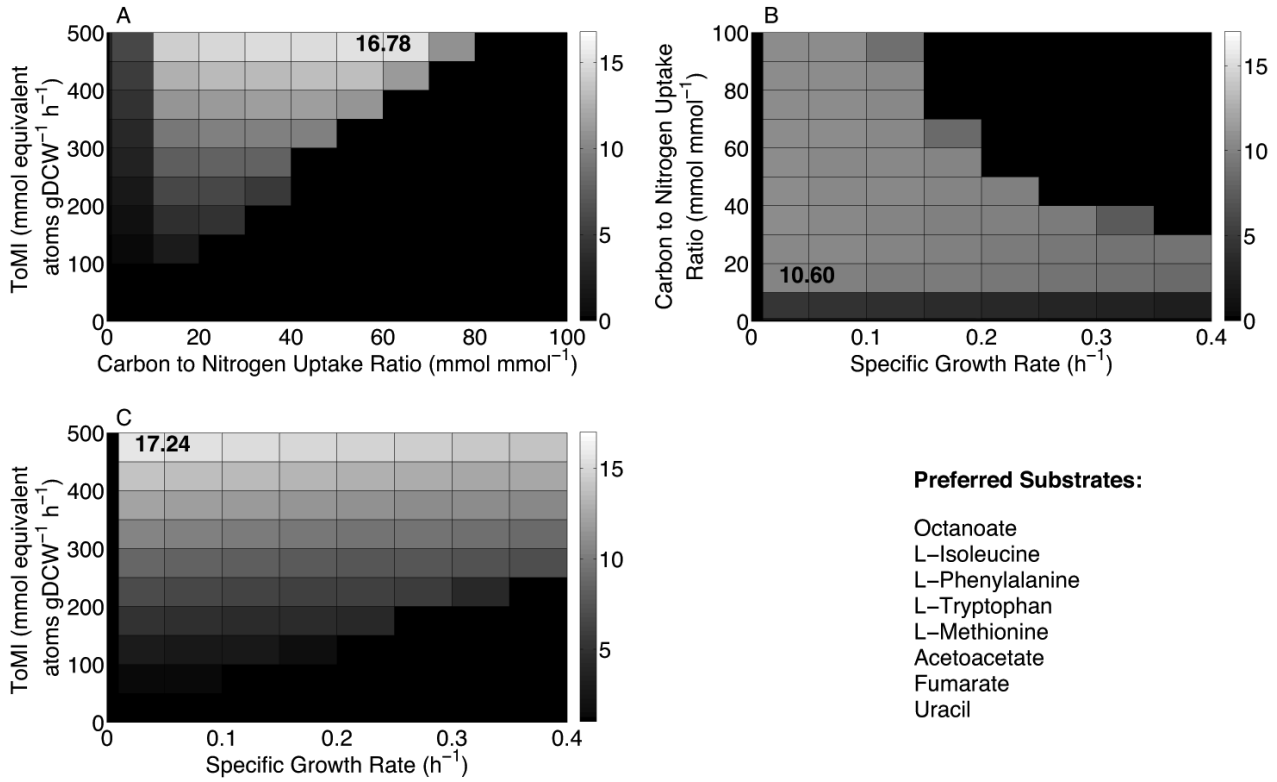

Figure 3. Production of mcl-PHA from the *P. putida* KT2440 genome-scale model. (A) Varied ToMI and CNR given a constant specific growth rate of 0.2 h^{-1}. (B) Varied CNR and specific growth rate given a constant ToMI value of 300 mmol equivalent atoms gDCW^{-1} h^{-1}. (C) Varied ToMI and specific growth rate given a constant CNR of 20 mmol mmol^{-1}. Also given is a list of preferred substrates found from ToMI-FBA simulations given a specific growth rate of 0.2 h^{-1}, ToMI of 300 mmol equivalent atoms gDCW^{-1} h^{-1}, and CNR of 20 mmol mmol^{-1}. The maximum values of each plot are given.

3.4. Case Study 4: Host selection for artemisinate production

The need for more effective antimalarial therapies led to the pursuit of artemisinin-based combination therapies, where artemisinate is a key drug. Artemisinin is a naturally derived product; however, the high price and low availability of this plant-derived antimalarial drug motivated investigation into production by an engineered MCF. In this regard, Martin et al. [55] first reported the production of amorphadiene, the precursor for artemisinate production, using engineered *E. coli* that expressed the mevalonate-dependent (MEV) pathway of *S. cerevisiae*. Tsuruta et al. [12] produced >0.25 g L^{-1} of amorphadiene in an optimized fed-batch, where HMG-CoA synthase and HMG-CoA reductase (two key genes in the MEV pathway) were replaced with homologs from *Staphylococcus aureus*. In addition, Ro et al. [47] introduced a cytochrome P450

monooxygenase (CYP71AV1) from *A. annua* to an engineered *S. cerevisiae* to enable the production of artemisinate from the precursor, amorphadiene in the same host. In this case study, the ToMI-FBA algorithm was applied to modified genome-scale models of *E. coli* K12 MG1655 (iAF1260) [42], *S. cerevisiae* (iND750) [40], *B. subtilis* (iBsu1103) [46], and *Synechocystis* PCC6803 (iJN678) [41] to determine which host is superior for producing artemisinate. All genome-scale models were modified to express the artemisinate pathway (Figure 1d). As a result of this pathway addition,

Table 1. Average ToMI-FBA reaction fluxes[*] of the isobutanol pathway installed in the iBsu1103 model of *B. subtilis*.

Reaction	Minimal Medium + L-Valine		Complex Medium	
	Average Flux (mmol $gDCW^{-1}$ h^{-1})	Standard Deviation	Average Flux (mmol $gDCW^{-1}$ h^{-1})	Standard Deviation
(2) Pyruvate → Acetolactate + CO_2	7.984	1.291	9.6510	0.1229
Pyruvate + 2-Hydroxyethyl-ThPP ↔ Acetolactate + TPP	0.8845	1.291	2.042	0.05810
Acetolactate + NADPH + H^+ ↔ 2,3-Dihydroxy-isovalerate + NADP	8.868	4.452×10^{-3}	11.69	0.1657
2,3-Dihydroxy-isovalerate ↔ 2-Keto-isovalerate + H_2O	8.868	4.452×10^{-3}	11.69	0.1657
2-Keto-isovalerate → Isobutyraldehyde + CO_2	11.67	1.441×10^{-5}	11.87	5.837×10^{-3}
Isobutyraldehyde + NADH + H^+ ↔ Isobutanol + NAD	11.67	1.441×10^{-5}	11.87	5.837×10^{-3}
L-Valine [e] + H^+ [e] → L-Valine [c] + H^+ [c]	2.931	1.441×10^{-5}	0.2436	0.1725
L-Proline [e] + H^+ [e] → L-Proline [c] + H^+ [c]	0	0	1.049	0.02466
Propionate [e] + H^+ [e] → Propionate [c] + H^+ [c]	0	0	2.723	0.1824

[*] The ToMI-FBA reaction fluxes are the upper limits of metabolic flux, not what is expected experimentally. Comparing the ToMI-FBA reaction fluxes can identify favorable conditions for production of a targeted metabolite.

[1] In ToMI-FBA simulations, isobutanol production was maximized in FBA.

[2] The ToMI value was constrained to 300 mmol equivalent atoms $gDCW^{-1}$ h^{-1}, the specific growth rate was constrained to 0.2 h^{-1}, and the glucose uptake rate was constrained to 10 mmol $gDCW^{-1}$ h^{-1} in all simulations.

[3] The Average Flux and Standard Deviation were obtained from 10 independent simulations containing 100 iterations each.

[4] The "[e]" and "[c]" specify extracellular and cytosol compartments, respectively. If unspecified, all other compounds are assumed to be cytosolic.

amorpha-4,11-diene and artemisinate were introduced to the genome-scale models of the aforementioned organisms as new compounds. To determine the maximum artemisinate production by these potential hosts, the ToMI-FBA was applied at multiple constrained growth rates (from 0.1 to 0.5 h^{-1}) and ToMI values (from 0 to 500 mmol equivalent atoms $gDCW^{-1}$ h^{-1}). The ToMI-FBA results for each potential host are shown in Figure 5. Overall, *in silico* expression of the pathway in *B. subtilis* (iBsu1103) revealed a higher artemisinate production potential compared to the other hosts. To demonstrate, at ToMI and specific growth rate values of 0.2 h^{-1} and 200 mmol equivalent atoms $gDCW^{-1}$ h^{-1}, *B. subtilis* has the potential to produce ~ 14% more artemisinate than either of *E. coli* or *S. cerevisiae*. *Synechocystis* PCC6803 (iJN678) returned almost 25% less artemisinate production *in silico* than either of *E. coli* (iAF1260) or *S. cerevisiae* (iND750). While we cannot validate this simulation result experimentally, this case study shows a unique application of ToMI-FBA.

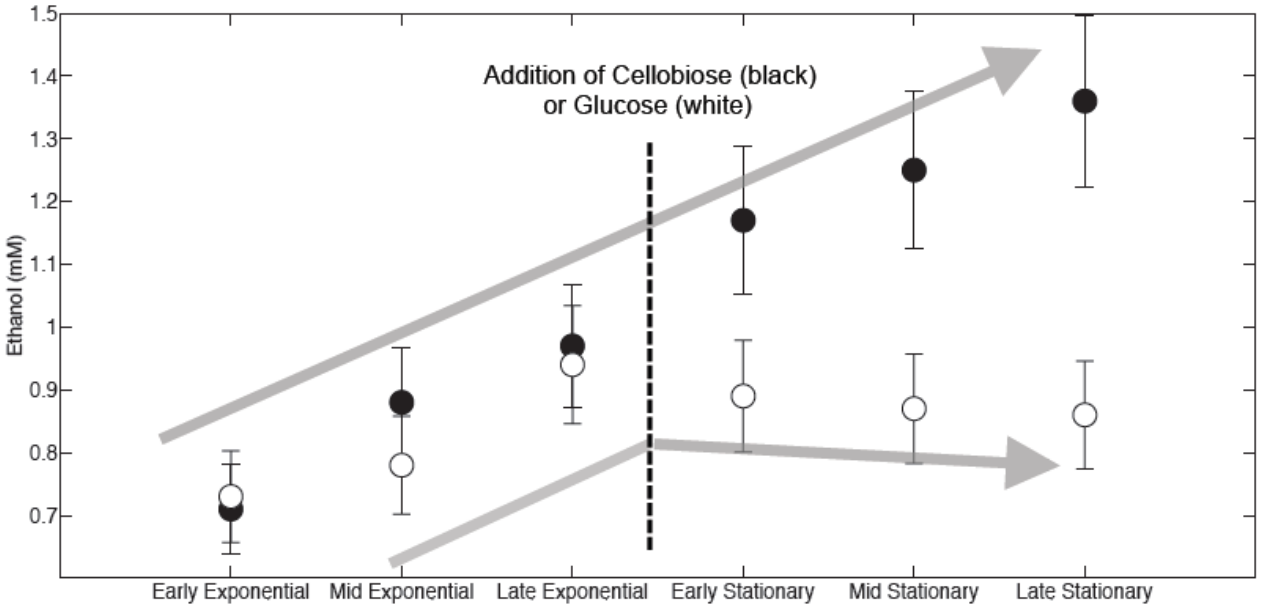

Figure 4. Experimental results showing the production of ethanol by *C. acetobutylicum* given the addition of glucose (white) or cellobiose (black) at the end of exponential growth.

A comparable simulation study can be run using a traditional FBA approach. To do this, one would do the following for all models: (i) constrain the growth rate to a specified value, (ii) constrain the artemisinate production rate to a specified value, (iii) unconstrain all membrane transport (and metabolite exchange) reactions, (iv) run pFBA to minimize total flux of the system. Then, one must compute the total atom flux of all metabolites transported into the metabolic network. This is done by calculating the product of the input flux and the number of atoms in the metabolite being transported (over all membrane transport reactions). This allows one to calculate the production of artemisinate per flux of atoms transported into the metabolic network. All models will return the same growth rate and artemisinate production rate. The optimum model will achieve this with the minimum input flux. ToMI-FBA solves this problem easily by doing the reverse. It allows the input atomic flux to be constrained (treating all membrane transporters equally) so the artemisinate production rate can be calculated directly and compared among different models.

4. Discussion

The ToMI-FBA approach has the ability to constrain the total atom influx of an *in silico* cellular model in order to evaluate metabolic activity. The ToMI constraint is unique in that it implements a constraint on multiple reactions simultaneously with the only requirement being that the sum of fluxes through those reactions equal a specified value. This approach removes bias commonly given to "larger" substrates that allow influx of additional carbon (e.g., glucose vs. cellobiose). The applications of ToMI-FBA are numerous, and those addressed in this research include culture medium design and host selection for optimized expression of engineered metabolic pathways.

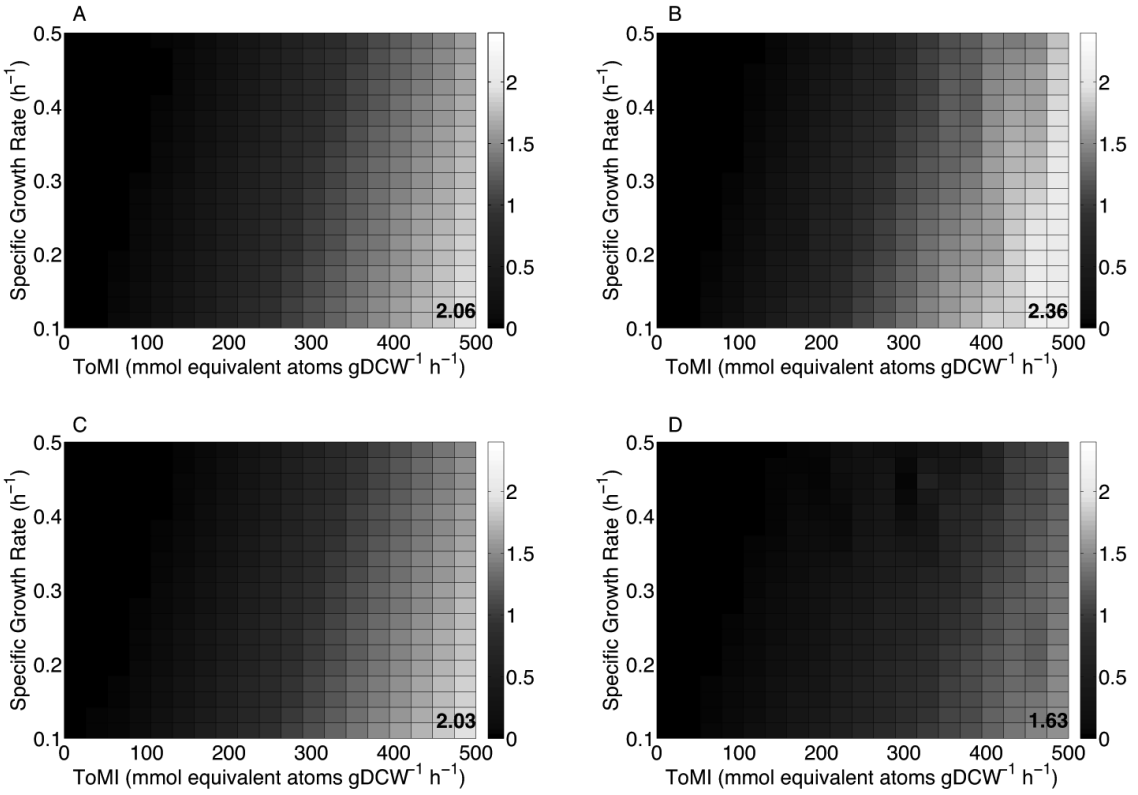

Figure 5. The maximum production of artemisinate (mmol gDCW^{-1} h^{-1}) from complex media as a function of ToMI and specific growth rate for the following models: (A) iAF1260 model of *E. coli*, (B) iBsu1103 model of *B. subtilis*, (C) iND750 model of *S. cerevisiae*, and (D) iJN678 model of *Synechocystis* PCC6803. The maximum values of each plot are given.

However, it is important to note that ToMI-FBA returns only the *potential* for product formation. ToMI-FBA operates by maximizing product formation as the objective of FBA (or pFBA). This does not mimic physical systems, as typically the growth rate of organism is maximized in nature (although several objective functions have been investigated in genome-scale modeling). Therefore, one possible future application of the ToMI-FBA might be combining it with another optimization problem (i.e., genetic manipulations) to formulate a bi-level optimization problem for maximizing

target product formation. However, significant metabolic engineering may be required to achieve the quantitative results returned by ToMI-FBA. This is particularly true for the case of host selection. Investigators must also take into account additional aspects such as: (i) the observed growth rate, (ii) the genetic toolsets available, and (iii) first-hand strain specific information and observations when selecting a host to express a targeted metabolic pathway.

ToMI-FBA will return the potential of possible hosts but not an estimate of the work required to achieve this potential. In addition, ToMI-FBA can be used to design optimal culture media formulations based on the potential for product formation. However, this too may require significant metabolic engineering to achieve optimal productivity. Additional points that should be emphasized about using ToMI-FBA for targeted pathway productivity predictions include the current unknown relationship between the specific growth rate and total membrane influx. Given relationships such as Fiures 2, 3, and 5, it is unknown what ToMI and specific growth rate combination will be observed in reality. For example the ToMI and specific growth rate of wild-type *E. coli* grown on glucose is much greater than that of *Synechocystis* PCC6803 grown autotrophically. In addition, the relationship between ToMI and the specific growth rate is not well understood and is likely organism-specific. In genome-scale metabolic flux models, this is likely a function of the biomass equation, which has been shown to have differing degrees of sensitivity to metabolic flux distributions in different models. In addition, ToMI-FBA cannot be used to predict physical characteristics for which mechanisms are not contained in the genome-scale metabolic flux model, such as product toxicity.

5. Conclusions

The ToMI-FBA approach has proven useful for screening culture medium components and even selecting microbial hosts that can maximize production of a targeted product. The CNR and SPF constraints provide a means for simulating metabolism under defined carbon-to-nitrogen uptake conditions as well under different culture medium pH conditions. Although achieving the quantitative production levels returned by ToMI-FBA may be unlikely, using ToMI-FBA results qualitatively is rational and has been shown in this research to result in increased product formation for three cases tested. ToMI-FBA should be used to design computational experiments that identify non-intuitive culture medium components and cellular responses. Ideally, ToMI-FBA will serve as a "first evaluation" for potential hosts and culture media formulations for newly designed metabolic pathways to be expressed by an engineered MCF. Additional uses of ToMI-FBA likely exist and should be explored in future research. In addition, the methodology of constraining ToMI and SPF presented in this research has numerous applications and can be used in conjunction with the similarly implemented FBrAtio constraint to design metabolic engineering strategies and determine metabolic potential.

Acknowledgements

Support for this research was provided by the National Science Foundation (awards NSF1243988 and NSF1254242) and the USDA (CSREES AFRI award 2010-65504-20346).

Conflict of Interest

The authors declare that there are no conflicts of interest related to this study.

References

1. Hanai T, Atsumi S, Liao JC (2007) Engineered synthetic pathway for isopropanol production in *Escherichia coli*. *Appl Environ Microbiol* 73: 7814–7818.
2. Atsumi S, Cann AF, Connor MR, et al. (2008) Metabolic engineering of *Escherichia coli* for 1-butanol production. *Metabolic Eng* 10: 305–311.
3. Connor MR, Liao JC (2008) Engineering of an *Escherichia coli* strain for the production of 3-methyl-1-butanol. *Appl Environ Microbiol* 74: 5769–5775.
4. McKenna R, Nielsen DR (2011) Styrene biosynthesis from glucose by engineered *E. coli. Metabolic Eng* 13: 544–554.
5. McKenna R, Pugh S, Thompson B, et al. (2013) Microbial production of the aromatic building-blocks (S)-styrene oxide and (R)-1,2-phenylethanediol from renewable resources. *Biotechnol J* 8: 1465–1475.
6. Moon TS, Dueber JE, Shiue E, et al. (2010) Use of modular, synthetic scaffolds for improved production of glucaric acid in engineered *E. coli*. *Metabolic Eng* 12: 298–305.
7. Tseng HC, Martin CH, Nielsen DR, et al. (2009) Metabolic engineering of *Escherichia coli* for enhanced production of (R)- and (S)-3-hydroxybutyrate. *Appl Environ Microbiol* 75: 3137–3145.
8. Ajikumar PK, Xiao WH, Tyo KE, et al. (2010) Isoprenoid pathway optimization for Taxol precursor overproduction in *Escherichia coli*. *Science* 330: 70–74.
9. Engels B, Dahm P, Jennewein S (2008) Metabolic engineering of taxadiene biosynthesis in yeast as a first step towards Taxol (Paclitaxel) production. *Metabolic Eng* 10: 201–206.
10. Scaife MA, Burja AM, Wright PC (2009) Characterization of cyanobacterial beta-carotene ketolase and hydroxylase genes in *Escherichia coli*, and their application for astaxanthin biosynthesis. *Biotechnol Bioeng* 103: 944–955.
11. Lemuth K, Steuer K, Albermann C (2011) Engineering of a plasmid-free *Escherichia coli* strain for improved in vivo biosynthesis of astaxanthin. *Microb Cell Fact*10: 29.
12. Tsuruta H, Paddon CJ, Eng D, et al. (2009) High-level production of amorpha-4,11-diene, a precursor of the antimalarial agent artemisinin, in *Escherichia coli*. *PloS One* 4: e4489.
13. Becker J, Wittmann C (2012) Bio-based production of chemicals, materials and fuels - *Corynebacterium glutamicum* as versatile cell factory. *Curr Opin Biotechnol* 23: 631–640.
14. Lindberg P, Park S, Melis A (2010) Engineering a platform for photosynthetic isoprene production in cyanobacteria, using *Synechocystis* as the model organism. *Metabolic Eng* 12: 70–79.
15. Hatzimanikatis V, Li C, Ionita JA, et al. (2005) Exploring the diversity of complex metabolic networks. *Bioinformatics* 21: 1603–1609.
16. Finley SD, Broadbelt LJ, Hatzimanikatis V (2009) Computational framework for predictive biodegradation. *Biotechnol Bioeng* 104: 1086–1097.
17. Henry CS, Broadbelt LJ, Hatzimanikatis V (2010) Discovery and analysis of novel metabolic pathways for the biosynthesis of industrial chemicals: 3-hydroxypropanoate. *Biotechnol Bioeng* 106: 462–473.

18. Fisher AK, Freedman BG, Bevan DR, et al. (2014) A review of metabolic and enzymatic engineering strategies for designing and optimizing performance of microbial cell factories. *Comput Struct Biotechnol J* 11: 91–99.
19. Lee SK, Chou H, Ham TS, et al. (2008) Metabolic engineering of microorganisms for biofuels production: from bugs to synthetic biology to fuels. *Curr Opin Biotechnol* 19: 556–563.
20. McEwen JT, Atsumi S (2012) Alternative biofuel production in non-natural hosts. *Curr Opin Biotechnol* 23: 744 – 750.
21. Jang YS, Park JM, Choi S, et al. (2012) Engineering of microorganisms for the production of biofuels and perspectives based on systems metabolic engineering approaches. *Biotechnol Adv* 30: 989–1000.
22. Atsumi S, Hanai T, Liao JC (2008) Non-fermentative pathways for synthesis of branched-chain higher alcohols as biofuels. *Nature* 451: 86–89.
23. Atsumi S, Higashide W, Liao JC (2009) Direct photosynthetic recycling of carbon dioxide to isobutyraldehyde. *Nat Biotechnol* 27: 1177–1180.
24. Smith KM, Cho KM, Liao JC (2010) Engineering *Corynebacterium glutamicum* for isobutanol production. *Appl Microbiol Biotechnol* 87: 1045–1055.
25. Jia X, Li S, Xie S, et al. (2011) Engineering a metabolic pathway for isobutanol biosynthesis in *Bacillus subtilis*. *Appl Biochem Biotechnol* 168: 1 – 9.
26. Chen X, Nielsen KF, Borodina I, et al. (2011) Increased isobutanol production in *Saccharomyces cerevisiae* by overexpression of genes in valine metabolism. *Biotechnol Biofuels* 4: 21.
27. Higashide W, Li Y, Yang Y, et al. (2011) Metabolic engineering of *Clostridium cellulolyticum* for production of isobutanol from cellulose. *Appl Environ Microbiol* 77: 2727–2733.
28. Orth JD, Thiele I, Palsson BO (2010) What is flux balance analysis? *Nat Biotechnol* 28: 245–248.
29. Varma A, Palsson BO (1994) Metabolic flux balancing - basic concepts, scientific and practical use. *Bio-Technol* 12: 994–998.
30. Reed JL, Palsson BO (2004) Genome-scale in silico models of *E. coli* have multiple equivalent phenotypic states: assessment of correlated reaction subsets that comprise network states. *Genome Res* 14: 1797–1805.
31. Henry CS, DeJongh M, Best AA, et al. (2010) High-throughput generation, optimization and analysis of genome-scale metabolic models. *Nat Biotechnol* 28: 977–982.
32. Devoid S, Overbeek R, DeJongh M, et al. (2013) Automated genome annotation and metabolic model reconstruction in the SEED and Model SEED. *Methods Mol Biol* 985: 17–45.
33. DeJongh M, Formsma K, Boillot P, et al. (2007) Toward the automated generation of genome-scale metabolic networks in the SEED. *BMC Bioinformatics* 8: 139.
34. Zakrzewski P, Medema MH, Gevorgyan A, et al. (2012) MultiMetEval: comparative and multi-objective analysis of genome-scale metabolic models. *PloS One* 7: e51511.
35. Hucka M, Finney A, Sauro HM, et al. (2003) The systems biology markup language (SBML): a medium for representation and exchange of biochemical network models. *Bioinformatics* 19: 524–531.
36. Schellenberger J, Que R, Fleming RM, et al. (2011) Quantitative prediction of cellular metabolism with constraint-based models: the COBRA Toolbox v2.0. *Nat Protoc* 6: 1290–1307.

37. McAnulty MJ, Yen JY, Freedman BG, et al. (2012) Genome-scale modeling using flux ratio constraints to enable metabolic engineering of clostridial metabolism in silico. *BMC Syst Biol* 6: 42.
38. Yen JY, Nazem-Bokaee H, Freedman BG, et al. (2013) Deriving metabolic engineering strategies from genome-scale modeling with flux ratio constraints. *Biotechnol J* 8: 581–594.
39. de Oliveira Dal'Molin CG, Quek LE, Palfreyman RW, et al. (2010) AraGEM, a genome-scale reconstruction of the primary metabolic network in *Arabidopsis*. *Plant Physiol* 152: 579–589.
40. Duarte NC, Herrgard MJ, Palsson BO (2004) Reconstruction and validation of *Saccharomyces cerevisiae* iND750, a fully compartmentalized genome-scale metabolic model. *Genome Res* 14: 1298–1309.
41. Nogales J, Gudmundsson S, Knight EM, et al. (2012) Detailing the optimality of photosynthesis in cyanobacteria through systems biology analysis. *Proc Natl Acad Sci U S A* 109: 2678–2683.
42. Feist AM, Henry CS, Reed JL, et al. (2007) A genome-scale metabolic reconstruction for *Escherichia coli* K-12 MG1655 that accounts for 1260 ORFs and thermodynamic information. *Mol Syst Biol* 3: 121.
43. Jones SW, Paredes CJ, Tracy B, et al. (2008) The transcriptional program underlying the physiology of clostridial sporulation. *Genome Biol* 9: R114.
44. Lewis NE, Hixson KK, Conrad TM, et al. (2010) Omic data from evolved *E. coli* are consistent with computed optimal growth from genome-scale models. *Mol Syst Biol* 6: 390.
45. Keating SM, Bornstein BJ, Finney A, et al. (2006) SBMLToolbox: an SBML toolbox for MATLAB users. *Bioinformatics* 22: 1275–1277.
46. Henry CS, Zinner JF, Cohoon MP, et al. (2009) iBsu1103: a new genome-scale metabolic model of *Bacillus subtilis* based on SEED annotations. *Genome Biol* 10: R69.
47. Ro DK, Paradise EM, Ouellet M, et al. (2006) Production of the antimalarial drug precursor artemisinic acid in engineered yeast. *Nature* 440: 940–943.
48. Senger RS, Papoutsakis ET (2008) Genome-scale model for *Clostridium acetobutylicum*: Part II. Development of specific proton flux states and numerically determined sub-systems. *Biotechnol Bioeng* 101: 1053–1071.
49. Baez A, Cho KM, Liao JC (2011) High-flux isobutanol production using engineered *Escherichia coli*: a bioreactor study with in situ product removal. *Appl Microbiol Biotechnol* 90: 1681–1690.
50. Blombach B, Riester T, Wieschalka S, et al. (2011) *Corynebacterium glutamicum* tailored for efficient isobutanol production. *Appl Environ Microbiol* 77: 3300–3310.
51. Li S, Wen J, Jia X (2011) Engineering *Bacillus subtilis* for isobutanol production by heterologous Ehrlich pathway construction and the biosynthetic 2-ketoisovalerate precursor pathway overexpression. *Appl Microbiol Biotechnol* 91: 577–589.
52. Follonier S, Panke S, Zinn M (2011) A reduction in growth rate of *Pseudomonas putida* KT2442 counteracts productivity advances in medium-chain-length polyhydroxyalkanoate production from gluconate. *Microb Cell Fact* 10*:* 25.
53. Tracy BP, Jones SW, Fast AG, et al. (2012) Clostridia: the importance of their exceptional substrate and metabolite diversity for biofuel and biorefinery applications. *Curr Opin Biotechnol* 23: 364–381.
54. Senger RS, Papoutsakis ET (2008) Genome-scale model for *Clostridium acetobutylicum*: Part I. Metabolic network resolution and analysis. *Biotechnol Bioeng* 101: 1036–1052.

55. Martin VJ, Pitera DJ, Withers ST, et al. (2003) Engineering a mevalonate pathway in *Escherichia coli* for production of terpenoids. *Nat Biotechnol* 21: 796–802.